

## Search for short-period acoustic waves with high-resolution 2D spectra<sup>(\*)</sup>

M. WUNNENBERG<sup>(1)</sup>, J. HIRZBERGER<sup>(1)(2)</sup> and F. KNEER<sup>(1)</sup>

<sup>(1)</sup> *Universitäts-Sternwarte - Geismarlandstraße 11, D-37083 Göttingen, Germany*

<sup>(2)</sup> *Institut für Geophysik, Astrophysik und Meteorologie  
Universitätsplatz 5, A-8010 Graz, Austria*

(ricevuto il 10 Giugno 2002; approvato il 7 Agosto 2002)

**Summary.** — The data for this contribution were taken in August 2000 with the “Göttingen” two-dimensional spectrometer in the VTT on Tenerife. Our spectrometer is based on two scanning Fabry-Perot Interferometers (FPIs). The non-magnetic Fe I 5434 Å line was observed in the quiet Sun at disk center. Time sequences of 41 min duration and with 25 s cadence were taken. Strictly simultaneously with the narrow-band FPI images (32 mÅ FWHM), broad-band images were recorded. The latter were reconstructed with speckle methods. With the known “true” broad-band object we are able to restore the narrow-band images as well. Our aim is to find propagating acoustic waves at short periods and small scales. The results obtained so far are presented and the prospects are discussed.

PACS 96.60.Mz – Photosphere, granulation.

PACS 01.30.Cc – Conference proceedings.

### 1. – Introduction

Numerical simulations of solar granulation (*e.g.* [1,2]) have shown that dynamic processes in the upper photosphere and the chromosphere (acoustic waves, shocks, etc.) are excited by granular motions. Observational evidence for a close relation between granular motions and acoustic waves was given by, *e.g.* [3] and [4]. The observational proof for the existence of small-scale events like shock waves is still missing although some evidences were found by [5] and [6]. Small-scale acoustic processes occur necessarily on short time scales. Hence, to study them, spectroscopic data with high spatial and temporal resolution are needed. We obtain these with the “Göttingen” two-dimensional spectrometer, which consists of two scanning Fabry-Perot Interferometers (FPIs).

---

<sup>(\*)</sup> Paper presented at the International Meeting on THEMIS and the New Frontiers of Solar Atmosphere Dynamics, Rome, Italy, March 19-21, 2001.

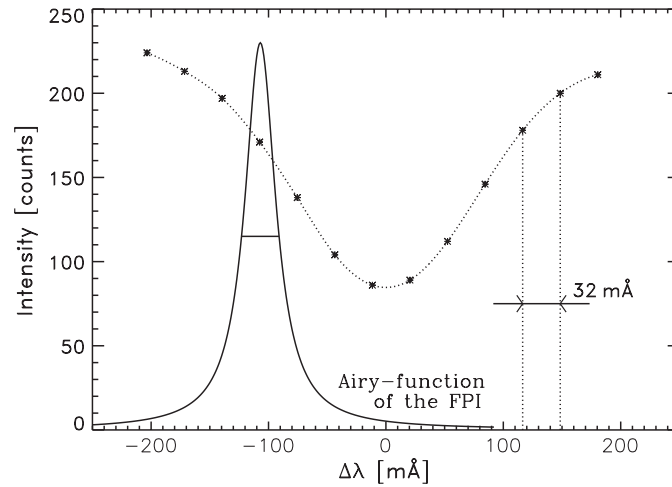


Fig. 1. – Line profile of Fe I 5434 Å. The asterisks show the observed spectral positions.

## 2. – Observations and data analysis

The data for this contribution stem from the “Göttingen” Fabry-Perot Interferometer mounted in the VTT at the Observatorio del Teide, Tenerife. They were taken on August 28, 2000 from quiet Sun at disk center. The set-up was essentially the same as described in [7], but instead of the polarimeter a glass block with the same optical length was used. The system works as a tunable narrow-band filter consisting of an interference filter (FWHM = 5 Å) centered at 5434 Å and two scanning etalons (FWHM = 200 mÅ, FWHM = 32 mÅ). The FPIs are mounted in the parallel beam to prevent flatness errors of the etalon surfaces affecting the data. We have obtained strictly simultaneously narrow-band scans through the non-magnetic Fe I line at 5434 Å and white-light images. The latter were taken through a broad-band filter (50–100 Å FWHM) centered at the same wavelength range. The iron line was scanned at 13 spectral positions and 8 images at each wavelength position were taken. The stepwidth was  $\Delta\lambda = 32 \text{ mÅ}$ , so that a spectral range of about  $\pm 200 \text{ mÅ}$  from the line center was scanned. The Airy-function of the FPI and the line profile is shown in fig. 1.

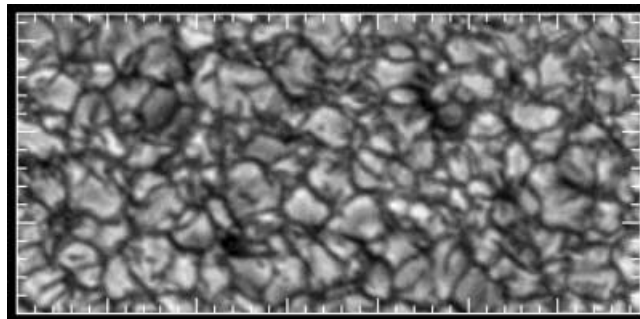


Fig. 2. – Speckle reconstructed broad-band image, distance of tickmarks:  $1''$ .

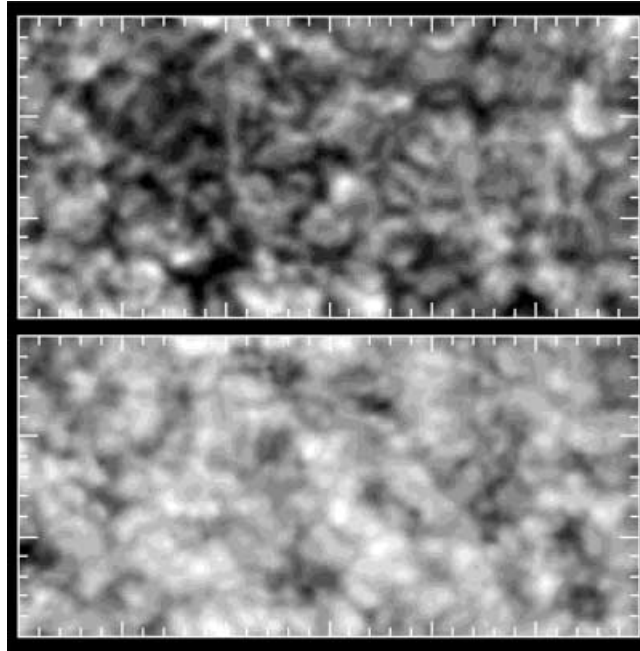


Fig. 3. – Intensity map (upper frame) and corresponding velocity map (lower frame) in the line center, distance of tickmarks:  $1''$ .

We have taken 100 scans containing 104 images each. The exposure time was 20 ms and the time interval between two scans was 25 s, *i.e.* the total length of the time series is about 41 min. The image scale on the CCDs is  $0.1''$  per pixel and the image size is  $384 \times 200$  pixel. All images were corrected for dark offset, flat fields and global image motion. Moreover, the narrow-band data were corrected for the transmission-curve of the interference filter.

In order to restore image degradation by the Earth's atmosphere (seeing), post facto reconstruction methods were used: the broad-band images were reconstructed by speckle interferometric techniques as described in [8]. The Fried parameters of our time series vary in the range of  $9 \text{ cm} < r_0 < 12 \text{ cm}$ . A speckle reconstructed granulation image is shown in fig. 2.

Since the broad-band and narrow-band images were exposed strictly simultaneously, we assume that the optical transfer function (OTF) is the same for both. With this knowledge the narrow-band images can be restored as well (see [9]). After reconstruction, we get a line profile at each pixel in the field of view for each scan. From these line profiles velocities have been calculated from the Doppler shifts at line center. We obtained the absolute values of the velocities by assuming that the average velocity in the field of view is zero. For each velocity map the corresponding intensity map was calculated (line center intensity). Examples of an intensity map and the corresponding velocity map are shown in fig. 3.

The 100 speckle reconstructed broad-band images were correlated and destretched using “local correlation techniques” (cf. [10]). This gives a three-dimensional data cube for the intensity depending on two spatial coordinates and the time,  $I_{bb}(x, y, t)$ . The

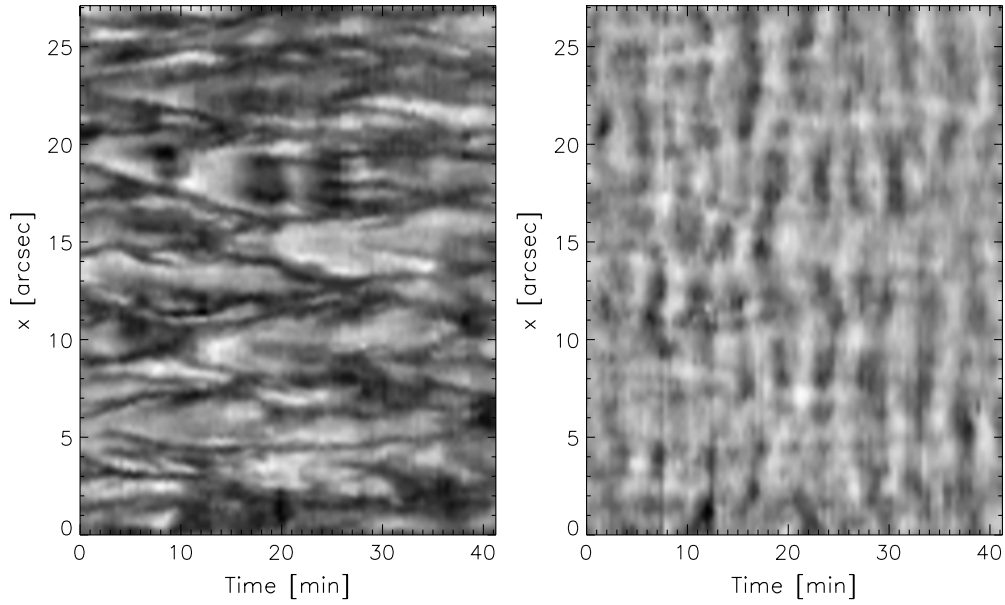


Fig. 4. –  $x$ - $t$  diagrams for the broad-band images (left) and the line center velocities (right).

resulting shifts and distortions were also applied to the line center velocity and intensity maps giving data cubes  $I_0(x, y, t)$  and  $V_0(x, y, t)$ .

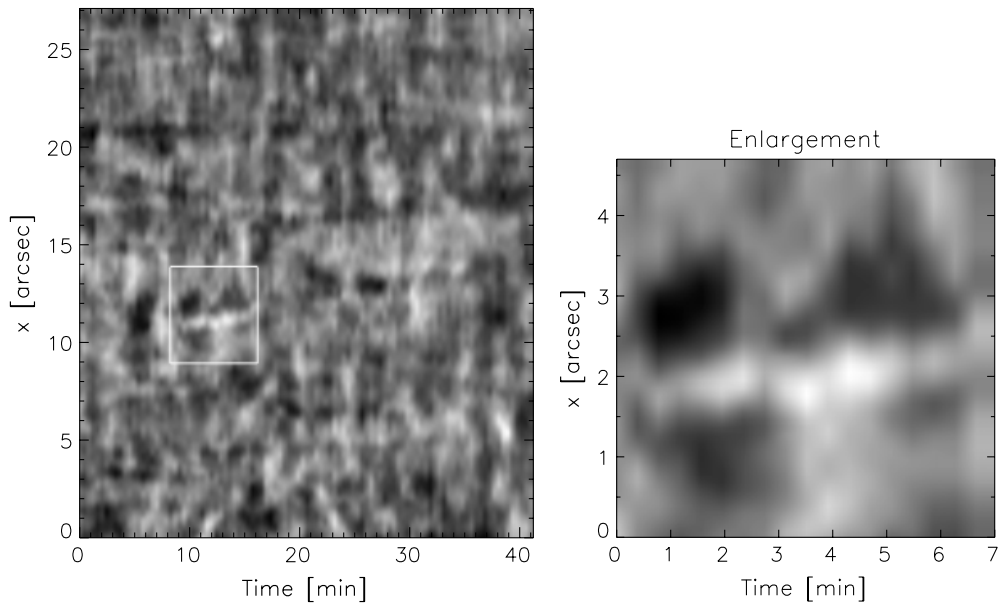


Fig. 5. –  $x$ - $t$  diagram for the line center intensities.

### 3. – Preliminary results

From movies of these data cubes one can see that the dynamics in the line center is significantly deviating from that in the continuum (granulation). To show this, we made time slices in order to get  $x-t$  diagrams. The evolution of granules can be seen on the time slice of the broad-band images (fig. 4, left).

In the line center (see the  $x-t$  diagram in fig. 4, right) the main contribution to the velocities comes from the 5 min oscillations. But we search for dynamic processes on shorter time scales. The line center intensity is a more suitable parameter searching for them because the 5 min oscillations are less pronounced there. In the corresponding  $x-t$  diagram (fig. 5) several conspicuous brightnings can be seen. The brightness of these phenomena is significantly above the noise level of our data. The enlargement shows one of these brightnings recurring twice within two minutes. In the  $x-t$  diagram of the white-light images (fig. 4, left) one can see that these brightnings occur above the edge of a tiny but increasing granule.

We have seen that dynamic processes on short time scales can be detected in our data. We have presented preliminary results here and we are working on a more detailed physical interpretation to be presented in the near future.

\* \* \*

Financial support by the Deutsche Forschungsgemeinschaft (grant KN 152/24-1) and by the Austrian Fonds zur Förderung der wissenschaftlichen Forschung (Erwin-Schrödinger-Stipendium J-1976 PHY) is gratefully acknowledged. The Vacuum Tower Telescope is operated by the Kiepenheuer-Institut für Sonnenphysik in Freiburg (Germany) at the Spanish Observatorio del Teide of the Instituto de Astrofísica de Canarias in Tenerife.

### REFERENCES

- [1] SKARTLIEN R., STEIN R. F. and NORDLUND A., *Astrophys. J.*, **541** (2000) 468.
- [2] WEDEMEYER S., FREYTAG B., STEFFEN M. and HOLWEGER H., *AGM*, **17** (2000) 01.
- [3] RIMMELE T. R., GOODE P. R., HAROLD W. and STEBBINS R. T., *Astrophys. J.*, **444** (1995) 119.
- [4] HOEKZEMA N. M., BRANDT P. N. and RUTTEN R. J., *Astron. Astrophys.*, **333** (1998) 322.
- [5] NESIS A., BOGDAN T. J., CATTANEO F., HANSLMEIER A., KNÖLKER M. and MALAGOLI A., *Astrophys. J.*, **399** (1992) 99.
- [6] SOLANKI S. K., RÜEDI I., BIANDA M. and STEFFEN M., *Astron. Astrophys.*, **308** (1995) 623.
- [7] KOSCHINSKY M., KNEER F. and HIRZBERGER J., *Astron. Astrophys.*, **365** (2001) 588.
- [8] DE BOER C.R., *Speckle-Interferometrie und ihre Anwendung auf die Sonnenbeobachtung* (Dissertation, Universität Göttingen) 1993.
- [9] KRIEG J., WUNNENBERG M., KNEER F., KOSCHINSKY M. and RITTER C., *Astron. Astrophys.*, **343** (1999) 983.
- [10] NOVEMBER L. J. and SIMON G. W., *Astrophys. J.*, **333** (1988) 427.